# A rheological model for spheroids including extra-cellular matrix

Claude Verdier, Liviu Iulian Palade

Cite this: DOI: 00.0000/xxxxxxxxxx

# A rheological model for spheroids including extra-cellular matrix†

Claude Verdier,*[a] and Liviu Iulian Palade[b]

Received Date
Accepted Date

DOI: 00.0000/xxxxxxxxxx

The rheology of spheroids has been studied intensively recently and it was shown that the presence of the extra-cellular matrix (ECM) can have significant effects on the overall behaviour of these biological systems. Collagen-I can indeed be a proxy between cells and bring new intriguing effects, as its content increases. To investigate these effects further, a two-phase emulsion model is proposed including interactions between cells and the ECM. Starting with the single cell and collagen individual viscoelastic properties, the model can be tested against previously obtained data for spheroids. The model has interesting features and capabilities for it covers a variety of behaviours and uses fitting parameters such as collagen and cell concentration, as well as adhesion energy. It is shown that the final intercellular collagen content can be large as compared to the initial one, and that this increase in collagen content induces a larger packing of cells, together with a larger adhesion energy.

## 1 Introduction

Spheroids are very interesting 3D biological systems, and good candidates to describe tumours[1]. Although there has recently been a growing interest to investigate how they react to osmotic pressures or mechanical forces[2–6], their mechanical properties are not yet satisfactorily understood. Indeed, cells packed together correspond to a concentrated suspension with shear–dependent viscosity or viscoelastic behaviour[7], but the extracellular matrix embedded into the system, or secreted by cells makes the picture harder to describe. In addition cells are viscoelastic, in particular cancer cells are known to exhibit different mechanical signatures like a larger deformability[8–10] or a frequency–dependent glass transition depending on invasiveness or grade[11–13]. Moreover their mechanical behaviour depends largely on the environment, in particular they rigidify when in contact with a substrate with higher stiffness, i.e. they are mechanosensitive[6,14]. They can also transform when the microenvironment is mechanically altered[15]. A few studies have focused on the effect of extra-cellular matrix (ECM) and its potential role to change the rheology of the spheroids. In particular, ECM can be considered as a proxy[16] acting as a porous material drained by water or the culture medium present in the spheroid[17]. But the influence of a larger collagen content may allow the building up of a new microstructure made of interconnected fibers also responsible for the larger mechanical moduli observed[18]. It is definitely accepted that the whole spheroid exhibits a viscoelastic pattern, due to the presence of cells embedded within the ECM – a gel-like system – with liquid medium. Probably the best way to model the behaviour of such spheroids is to consider the ECM–water surrounding medium as a gel with viscous and elastic properties. Such ECM properties have been studied extensively in the literature in the linear and nonlinear regimes, showing the role of cross–linking effects[19], negative normal stresses[20], concentration-dependent shear moduli[21], nonlinear rheology following pre–stress protocols[22], and the insensitivity of MR based diffusion measurements to various collagen hydrogels[23]. In addition the gel biopolymers enable cells to bind or adhere within connective tissues or other situations to allow stress transfer[24].

In this work we propose to study spheroids consisting of two phases, i.e. the ensemble of cells and the collagen matrix. We use the matrix mechanical properties as well as individual cell properties in contact with a similar environment, that is to say when they are surrounded by other cells. Then we consider a viscoelastic emulsion model, valid for large concentrations in order to predict the whole spheroid rheology. This is carried out in detail by varying the model parameters. Finally we optimize these parameters to rationalize previous results[18] obtained for spheroids containing an excess of collagen.

## 2 Materials and methods

### 2.1 Collagen

Collagen was prepared according to the manufacturer's protocol (Corning). Rat tail collagen I was mixed with PBS (1X) and NaOH (1M) was added at 4°C until the correct pH was obtained (7.4). Then it was let to polymerise at 37°C for 30 minutes. These collagen properties were measured as described in previous work[25]. Briefly, classical rheometry tests at 37°C using parallel plate geometry (20mm-diameter) were carried out in oscillatory shear mode in the [0.03Hz-10Hz] range. Then experiments using AFM in force modulation mode were carried out following a previous method[26,27] using indentation of a flat collagen layer (in PBS) with a pyramid AFM tip (Bruker, MLCT, half angle $\theta \sim 20°$). An initial indentation $\delta_0$ was applied, followed by small oscillations in the linear regime ($\delta << \delta_0$), thus allowing to measure the

[a] Address, Université Grenoble-Alpes, CNRS, LIPhy, 38000 Grenoble, France. Tel: 33 4 76 63 59 80; E-mail: claude.verdier@univ-grenoble-alpes.fr
[b] Address, CNRS, LaMCoS UMR 5259 & Pôle de Mathématiques, INSA-Lyon, Université de Lyon, 69621 Villeurbanne, France. E-mail: liviu-iulian.palade@insa-lyon.fr

complex shear moduli $G^*(\omega) = \frac{1-\nu}{3\delta_0 \tan\theta}\left\{\frac{F^*}{\delta^*} - i\omega b(0)\right\}$, where G*=G'+iG", G' and G" are respectively the elastic and loss shear moduli, $\nu$ is the Poisson ratio ($\nu \sim 0.5$), $F^*$ and $\delta^*$ are the complex force and indentation, and the last term is the drag on the surrounding liquid, with b(0) being a coefficient containing the geometry of the system as well as the fluid viscosity[26]. Using these complementary experiments, the range [0.03Hz-1kHz] was covered. Note that the hypothesis $\nu \sim 0.5$ involves the fact that poroelastic effects are neglected which is often the case ($\nu \sim 0.49$, see work on PolyAcrylamide gels[28]). However, this can become an important factor for some gels, in particular when analyzing relaxation curves for long times, as in the case of hydrogels exhibiting $\nu \sim 0.4$[29]. In the present study, since fast solicitation frequencies are used, it is known that the fluid does not move relative to the microstructure if $f > \frac{1}{2\pi}(\xi/L)^2 G/\eta$, where $\xi$ is the pore size, L the typical contact radius in the experiment, G and $\eta$ are the shear modulus and viscosity of the gel[30,31]. Here using $\xi$=10 nm[5], with L∼500 nm typically in our experiments, and accounting for the collagen properties $0.7\ s^{-1} < G/\eta < 1.4\ 10^4\ s^{-1}$, we find that frequencies larger than ∼ 1Hz are required (worst case), which is true in our AFM experiments. This argument is further enhanced by checking the good correspondence between classical rheology and AFM data.

### 2.2 Cells

T24 cells (epithelial bladder cancer line) were cultured in RPMI medium with 10% FBS and 1% penicillin-streptomycin. These cells have been described before and their properties were previously found to depend on the environment, i.e. the substrate. In some cases, corrections depending on substrate stiffness need to be made[32]. Here we chose to measure T24 cell properties as if they were in contact with other cells, like in a real spheroid. The best possible way to do so is to form a spheroid (see description below) and approach a small AFM tip close to the surface, where cells are located. In such a case, no substrate corrections were needed since the environment consists of cells themselves. Such AFM measurements were carried out with a pyramidal tip (Bruker, MLCT, half angle $\theta \sim 20°$) for their viscoelastic shear moduli G' and G" at 37°C (same method as above). It was indeed important to find a relevant micro–environment for these cells, like in a real spheroid.

### 2.3 Spheroids

Spheroids were prepared in 15$\mu$L hanging droplets containing 5,000 T24 cells in culture medium including small amounts of collagen (initial concentration $c_0$ = 0 or 0.01 mg/mL or 0.03 mg/mL) as described previously[18]. This method allows cells to accumulate ECM without having too much collagen around the spheroids, which would render AFM measurements more difficult. A spheroid was formed after three days. Spheroids were transferred into a Petri dish for AFM measurements at 37°C. A large tipless cantilever (Nanosensors, TL-NCL model, length 225 $\mu$m, width 38 $\mu$m[6]) was chosen for these measurements in force modulation mode, in order to make a plane-spherical contact. Viscoelastic data was obtained in the range [1Hz-1kHz]. The other spheroids were kept for confocal microscopy imaging.

## 3 Properties of the collagen matrices

After collecting data from classical rheology and AFM, results were plotted on the same graph, as a function of frequency. Matching of the two types of experimental results was found to work nicely as previously shown for PolyAcrylamide samples[27]. Such results are shown in Fig. 1. A typical power-law behaviour[33] was found for both G' and G" at different collagen concentrations (c=1 mg/mL, 2 mg/mL, 4 mg/mL) in the range [0.05Hz-10 Hz] and both G' and G" increased faster in the high frequency range. Note that the measured values of the moduli were usually smaller as compared to cell's values[6]. Finally fitting of the data was achieved using simple power-laws as described below.

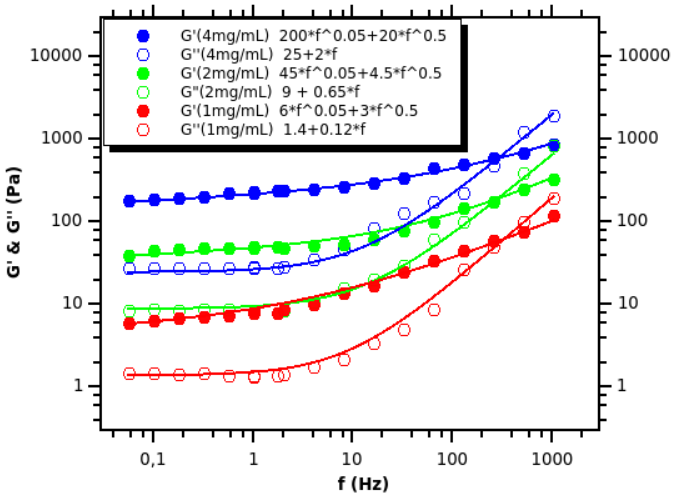


Fig. 1 Rheological properties of the collagen matrix for three concentrations (c = 1mg/mL, 2 mg/mL and 4mg/mL). Data are collected from classical rheology (0.01 Hz-10 Hz) and AFM rheology (1 Hz-1 kHz).

## 4 Cell properties

To investigate cell rheology, it was necessary to consider cells in the proper environment as it is known that the micro–environment plays a role on their cytoskeleton organization, therefore changes cellular mechanical properties[6,14]. Cells within a spheroid are surrounded by other cells and the ECM therefore it is convenient to use such a micro–environment[12]. Unfortunately, using AFM, it is hard to have access to the cell mechanical properties within the tissue, unlike when using other techniques such as bead tracking microrheology[34]. Here we preferred to use cell properties (T24 epithelial bladder cancer cells) obtained when in contact with similar cells, i.e. in the real spheroid. Fig. 2 below represents the G' and G" moduli obtained for cells located on the spheroid's periphery, as suggested before[12]. This is the closest representation of the micro–environment experienced by cells inside the spheroid. The frequency range was chosen from 1 Hz to 1 kHz using three points per decade. The cell behavior is a bit different from previous measurements of such T24 cells on rigid substrates, or on an endothelial substrate[32]. Indeed the plateau

for G' at low frequencies is replaced by a frequency-dependent modulus with a small slope $\sim 0.17$ (see modeling below). As for the G" modulus, it is similar to previous data[32].

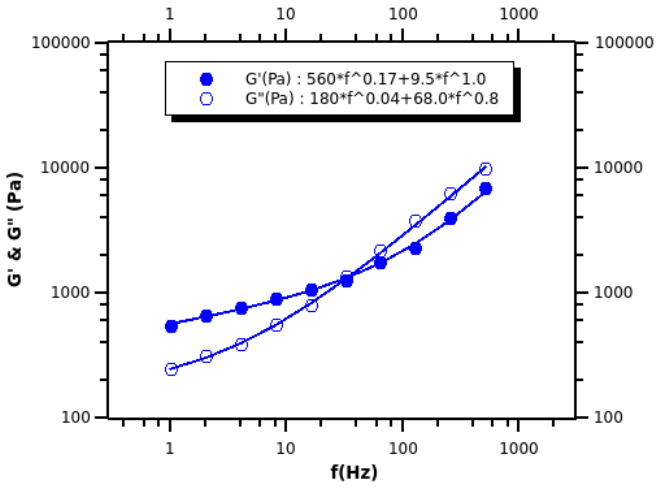


Fig. 2 Rheological data of a T24 cell, measured at the surface of the spheroid, as a close representation of the cell's environment. Average of N=20 measurements, using 10 spheroids at $c_0$=0.01mg/mL.

## 5 Two-phase model with interfacial tension

### 5.1 Emulsion model

Our starting point is Palierne's seminal work published in the early 90s[35,36]. This two–phase model designed for polymeric or viscoelastic systems requires the knowledge of complex shear moduli obtained for small deformations, i.e. in the linear regime. The model has been used mainly for two–phase polymeric systems (see for example the works on polymer blends[37]). Nevertheless it may be used for materials such as gels or cellular media exhibiting known viscoelastic properties. Here the medium, i.e. the collagen gel, has a characteristic complex modulus $G^*_m(\omega)$ whereas the inclusions (the cells) have modulus $G^*_i(\omega)$. The volume fraction of the inclusions is $\phi$ (thus volume collagen concentration is 1 - $\phi$ inside the spheroid) but different inclusions may be considered with different sizes and concentrations (in case of heterogeneous sizes). Here we assumed that only cells with a typical radius $R$ coexist, which is usually the case since cell size is roughly constant. In this case, $G^*(\omega)$, the average modulus of the spheroid, i.e. cells embedded in the collagen matrix, is written as, in the case of non-diluted emulsions[35]:

$$G^*(\omega) = G^*_m(\omega)\,\frac{1+3\phi H^*(\omega)}{1-2\phi H^*(\omega)} \qquad (1)$$

where the function $H^*(\omega)$ is defined as:

$$H^*(\omega) = \frac{\frac{4\alpha}{R}[2G^*_m(\omega)+5G^*_i(\omega)]+[G^*_i(\omega)-G^*_m(\omega)]D^*(\omega)}{\frac{40\alpha}{R}[G^*_m(\omega)+G^*_i(\omega)]+[2G^*_i(\omega)+3G^*_m(\omega)]D^*(\omega)} \qquad (2)$$

where we introduced $D^*(\omega) = 16G^*_m(\omega)+19G^*_i(\omega)$.

In this formula, $\alpha$ is the interfacial tension and may be considered here as an interaction energy per unit surface between cells and the matrix. It will be significant when cells adhere a lot to the matrix or are able to make a sufficiently large number of bonds. This may possibly be the case for high collagen content. Note that for the case of dilute emulsions, Eq.2 is different and should be replaced by $G^*(\omega) = G^*_m(\omega)(1+\frac{5}{2}\phi H^*(\omega))$. In particular, this allows to recover the usual Einstein's formula[38] for two Newtonian fluids.

To summarize, we could use this model based on the cell properties $G^*_i(\omega)$ determined previously and the gel properties $G^*_m(\omega)$, known for different collagen I concentrations. Note that the collagen concentration c (in mg/mL) is unknown within the spheroid, and similarly $\phi$, the cell volume concentration is to be determined. $\phi$ should be large since most of the spheroid is made of cells, and one could expect the ECM content to be possibly in the range 1-15%[5], assuming that cells make their own matrix. The other adjustable parameters are $\alpha$, the adhesion energy per unit area (in N/m), and $R$ the cell radius, but the latter one is known since such T24 cells usually have a radius of $10\mu$m $\pm$ $1\mu$m.

In a first approximation, we noticed that collagen moduli $G'_m$ and $G''_m$ are much smaller (an order of magnitude or more) than the corresponding cell moduli $G'_i$ and $G''_i$. Therefore, we could neglect the viscoelastic part in Eq (1). This implies that $D^*(\omega) \sim 19G^*_i(\omega)$ and $H^*(\omega) \sim \frac{1}{2}$ therefore $G^*(\omega) \sim G^*_m(\omega)\frac{1+1.5\phi}{1-\phi}$. So $G^*(\omega)$ scales with the matrix complex modulus $G^*_m(\omega)$, with the prefactor $\frac{1+1.5\phi}{1-\phi}$. Note that a small collagen content like 5% gives $\phi = 0.95$ therefore a prefactor of 48.5. Values of the prefactor are shown in the Table 1 below.

Table 1 Values of the prefactor

| $\phi$ | 0.05 | 0.1 | 0.3 | 0.5 | 0.7 | 0.9 | 0.95 |
|---|---|---|---|---|---|---|---|
| $\frac{1+1.5\phi}{1-\phi}$ | 1.13 | 1.28 | 2.07 | 3.5 | 6.83 | 23.5 | 48.5 |

This shows that even though the collagen modulus $G^*_m(\omega)$ is rather small (Plateau of G' around 200 Pa), as compared to cell's moduli (plateau of G' at 500 Pa), the amplification due to spherical inclusions such as cells can be large and could lead to the high values obtained in spheroids[18].

The formula also originates from analysis of the effect of the adhesion energy $\alpha$. If $\alpha/R$ becomes very small as compared to the other moduli (and collagen moduli are neglected vs. inclusions moduli) then the function $H^*(\omega)$ again becomes independent of $\alpha$ and is close to 1/2. At this stage, if we briefly compare with the results of our previous work[18], we notice that the moduli increase with collagen content (decreasing $\phi$). On the order hand, the previous equation predicts decreasing moduli. Therefore it seems important to consider the effect of all parameters: we consequently check the influence of $G^*_m(\omega)$, $\phi$, $\alpha/R$ upon the numerical results, while $G^*_i(\omega)$ remains fixed (Fig. 2).

### 5.2 Application to the rheology of spheroids

We have at our disposal the data from a previous study where collagen was added when making spheroids[18]. Three initial concentrations $c_0$ were used: 0 mg/mL, 0.01 mg/mL and 0.03 mg/mL.

This does not mean that the local collagen content (c) is the same when the spheroids are formed. Indeed spheroids were prepared in hanging droplets containing collagen; cells used it to adhere and spheroids exhibited a round shape. The same T24 cells were used for this study. Fig. 3 shows typical confocal microscopy images of such spheroids obtained using three initial collagen contents: $c_0$ = 0, 0.01 mg/mL and 0.03 mg/mL. As shown in the red channel, the reflectance of collagen was enhanced at higher collagen content, thus allowing to check the presence of collagen inside the spheroid. Cells (green channel, transfected with the LifeAct plasmid expressing actin–GFP) seemed to form nice round spheroids except for the first case where no collagen was added.

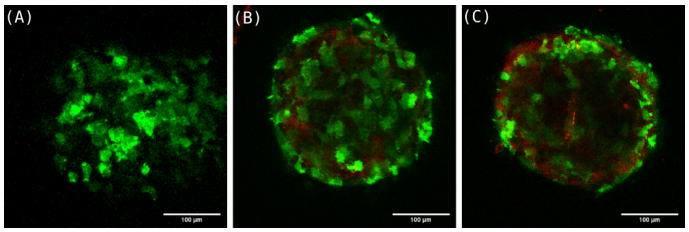


Fig. 3 Confocal microscopy images of spheroids prepared using T24 cells in hanging droplets, containing different initial collagen contents $c_0$ = 0mg/mL, 0.01mg/mL and 0.03mg/mL. Adapted from Tsvirkun *et al.*[18].

We will now model the different phases of the spheroid. The first one is collagen. Using the previous data in Fig. 1, it is found that the collagen behaviour varies according to power laws versus frequency f. Fits of our previous data give the respective formulae for the three contents, as also shown in Fig. 1. For $c$ = 4 mg/mL, we find $G'(f) = 200 * f^{0.05} + 20 * f^{0.5}$ and $G''(f) = 25 + 2 * f$. For $c$ =2 mg/mL, $G'(f) = 45 * f^{0.05} + 4.5 * f^{0.5}$ and $G''(f) = 9 + 0.65 * f$, and finally the lowest collagen content, $c$ = 1mg/mL, gives $G'(f) = 6 * f^{0.05} + 3 * f^{0.5}$ and $G''(f) = 1.4 + 0.12 * f$, where $f$ is in Hz, and $G'$, $G''$ are in Pascals (Pa). Remarkably, these power law exponents are independent of the concentration, so only the prefactors are different.

Similarly, we fitted the viscoelastic response of T24 cells, as shown in Fig. 2. The moduli behave as $G'(f) = 560 * f^{0.17} + 9.5 * f^{1.0}$ and $G''(f) = 180 * f^{0.04} + 68 * f^{0.8}$. T24 cells moduli exhibit a small slope at the lowest frequencies then the slope increases at higher ones.

Let us now consider the effects of the main parameters. Regarding the effect of modulus $G_i^*$, cells are assumed to have the behaviour depicted in Fig. 2 so this modulus is fixed. Then the values of the collagen modulus $G_m^*$ can be changed depending on its content (c in mg/mL) within the spheroid (see Fig. 1). Finally, the roles of the cell content ($\phi$) and the adhesion energy per unit area ($\alpha/R$) will be studied.

### 5.2.1 Effect of collagen matrix within the spheroid

Here we consider the case $\phi$=0.8 which corresponds to typical cell volume concentration, as seen for example in Fig. 3. For this case, we used $\alpha$=10.0 mN/m with $R = 10\,\mu$m. Plots of G' and G" are shown in Fig. 4.

As expected, spheroids moduli increase with collagen content,

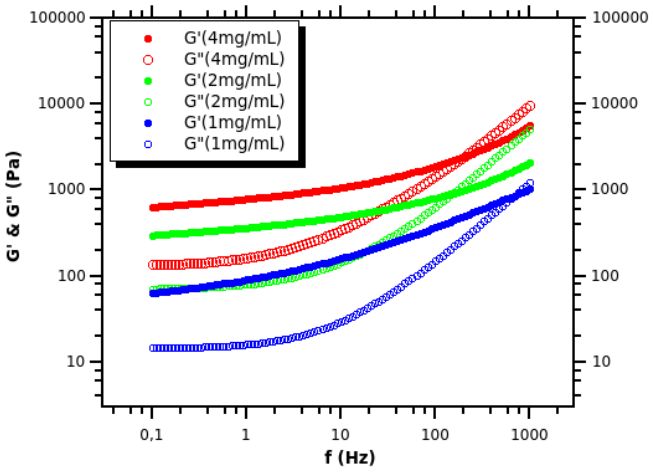


Fig. 4 Predictions of the two–phase emulsion model for 80% cell volume concentration, $\alpha/R$=$10^3$ Pa, at collagen contents $c$ = 1mg/mL, 2mg/mL and 4mg/mL.

as could be seen by inspection of formulae (1-2), where the collagen complex viscoelastic modulus $G_m^*(\omega)$ appears as a prefactor. It is found that the resulting properties of the spheroid are in the range of the data previously reported[18], and this will be studied further below.

### 5.2.2 Role of cell concentration

Next we studied the role of cell concentration. Usually, in spheroids, cells are closely packed but the presence of collagen, as seen in confocal microscopy (Fig. 3) suggests that the intercellular spacing can be modified. It has been estimated that the ECM content can sometimes reach $\sim$ 15% in cases where cells make their own ECM[5]. Therefore, we selected typical concentrations between 0% and 20% for the collagen gel, leading to cell concentrations between $\phi$ = 0.8 and $\phi$ = 1. For this case we used a low content of collagen (c = 2mg/mL) and $\alpha/R$=$10^3$ Pa. Simulations are shown in Fig.5. It can be concluded that cell concentration has an important effect on the results, especially due to the large difference between matrix and cell's moduli.

### 5.2.3 Effect of adhesion energy between cells and the matrix

Regarding the effect of the adhesion energy, we chose to study realistic values $\alpha$ of 0.3, 3, 30, and 300 mN/m at cell density $\phi$=0.9, and medium collagen content properties corresponding to c = 2mg/mL. This is shown in Fig. 6.

To summarize results from Fig. 6, it appeared that the role of $\alpha/R$ was important, for the chosen parameters and the values of the current viscoelastic parameters. This role became more important at lower frequencies where it was found that higher values of the adhesion energy increased the values of G' and G", in particular enhancing the formation of a plateau (in G') at low frequencies. Increasing the adhesion energy also increased the transition frequency (crossing between G' and G"). Thus, the more important the adhesion, the more elastic the spheroids became.

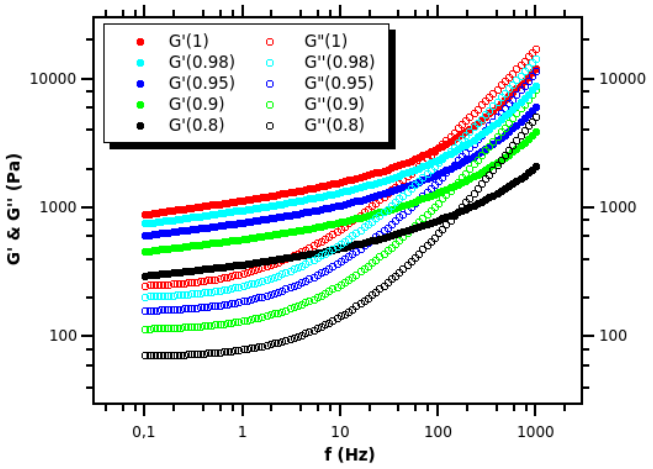


Fig. 5 Predictions of the two–phase emulsion model for various cell concentrations $\phi$ = 0.8, 0.9, 0.95, 0.98, 1, $\alpha/R$=$10^3$ Pa, at collagen content c = 2mg/mL.

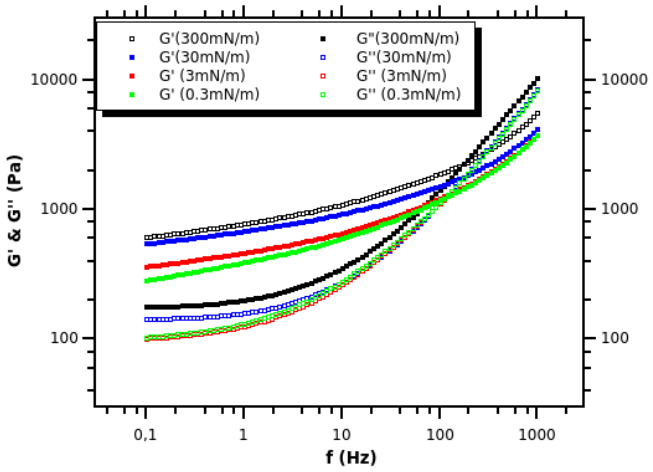


Fig. 6 Predictions of the two–phase emulsion model for various adhesion energies 0.3-3-30-300 mN/m, with $R$=10 $\mu$m, collagen content c = 2mg/mL, and $\phi$=0.9.

### 5.2.4 Optimizing emulsion model parameters for real spheroids

Finally, real spheroid properties were considered within the [1Hz-1kHz] range as previously described using AFM microrheology in plane–sphere contact[18]. Measurements were carried out in a manner similar to the one proposed on tissues[39]. Measurements display typical slopes as a function of frequency. To fit the data, parameters were optimized as follows. We adjusted the concentration $\phi$ (typically between 0.5 and 1), the collagen concentration between 1 to 4 mg/mL, and the value of $\alpha/R$. Results are shown in Fig. 7. Fits were in very good agreement with experimental data, even though slight discrepancies between data and model predictions were noticed at low frequencies (in particular for $c_0$ = 0). Here is a summary of the parameters found, with a fixed value R = 10 $\mu$m.

- $c_0$ **= 0 mg/mL**. For this case, there is no collagen, but cells secrete their own Extracellular Matrix (ECM) therefore we found an optimal collagen concentration of c = 2 mg/mL, $\phi$=0.82 and a value of $\alpha$ = 30 mN/ml.
- $c_0$ **= 0.01 mg/mL.** We found that the optimal parameters are a collagen concentration c = 4 mg/mL, $\phi$=0.88, and $\alpha$ = 60 mN/m.
- $c_0$ **= 0.03 mg/mL**. We find an optimal collagen concentration c = 4 mg/mL with $\phi$=0.94 and $\alpha$ = 80 mN/m.

The table below summarizes these results:

For the case $c_0$ = 0 mg/mL, it is probably true that there is a certain amount of ECM, but cells appear not much in contact with each others, therefore an intercellular volume spacing of 18 % as predicted by the model seems to be a reasonable value. There is discrepancy in the data as mentioned before[18] because of this lack of adhesion leading to non spherical spheroids.

Table 2 Optimal parameters (R = 10$\mu$m)

| | | | |
|---|---|---|---|
| Initial collagen ($c_0$, mg/mL) | 0 | 0.01 | 0.03 |
| Optimal $\phi$ | 0.82 | 0.88 | 0.94 |
| Inter-cellular space (1 - $\phi$) | 0.18 | 0.12 | 0.06 |
| Collagen content (c, mg/mL) | 2 | 4 | 4 |
| Adhesion energy/unit area $\alpha$ (mN/m) | 30 | 60 | 80 |

For the other two cases, an optimal collagen concentration c = 4 mg/mL seemed to be a suitable number, in agreement with confocal microscopy (see large amounts of collagen in Fig. 3). Finally cells seemed to be more densily packed in the second case ($c_0$ = 0.03 mg/mL), meaning that collagen helps cells to bind and plays the role of an interstitial layer enhancing the microstructure as well as the viscoelastic properties.

## 6 Discussion

The rheological properties of spheroids are of great importance in order to understand how microstructural changes evolve in time, and how they can affect mechanics, possibly giving rise to invasion of tumours and/or the formation of metastasis. In addition, their growth is also a topic of major interest. Tumours grow and exert pressure on the environment through a process limited by the surrounding medium[40]. Earlier models considered spherical growth depending on the nutrients[41], but more sophisticated ones now use numerical tools to evaluate hoop stresses inside and at the periphery of the growing spheroid[5,42,43]. Interesting studies have shown the effect of collagen on such processes, in particular the micro–environment (or ECM) can become the signature of cancer progression and prognosis[44–46]. In this work, we investigated the role of collagen on the viscoelastic properties of spheroids grown during 3 days[18], in culture medium containing an excess of collagen I (various initial concentrations $c_0$ from 0 to 0.03 mg/mL). Using a former model particularly well adapted for viscoelastic behaviors, we studied the possible effects linked to ECM (collagen I) density, cell concentration and adhesion. This was assessed by modeling frequency–dependent individual cell

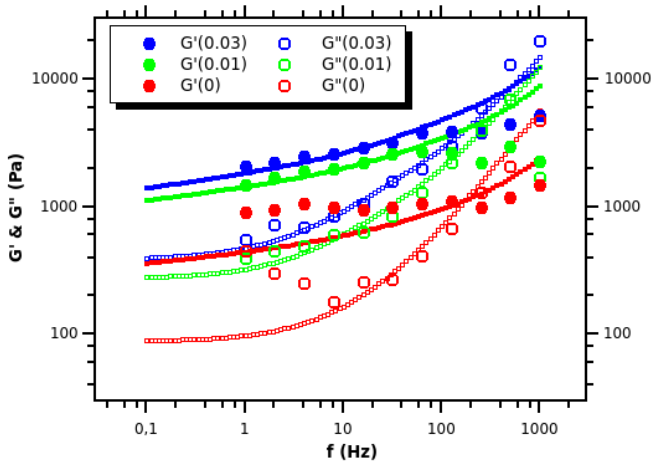


Fig. 7 Spheroid properties for three initial collagen contents $c_0$ = 0 mg/mL, 0.01 mg/mL and 0.03 mg/mL (data from previous work[18]) with using respective optimal parameters (c=2 mg/mL, $\phi$=0.82, $\alpha/R$=30mN/m), (c=4 mg/mL, $\phi$=0.88, $\alpha/R$=60mN/m) and (c=4 mg/mL, $\phi$=0.94, $\alpha/R$=80mN/m).

and collagen properties (Figs 1-2). Based on these properties, we used the two–phase emulsion model[35,36] able to recover the spheroid viscoelastic data.

The effect of collagen has already been shown to be a linker within spheroids using confocal microscopy (Fig. 3). Furthermore, we could also analyze its role on the overall spheroid's rheology as its concentration increases, using the two–phase emulsion model. It was shown that a high collagen content ($c$ varying from 1 to 4 mg/mL) enhanced the viscoelastic properties (Fig. 4). Another parameter, cell concentration ($\phi$), was seen to have a quite significant contribution to reinforce viscoelastic properties as well (Fig.5). Indeed, the initial simplified equation 1 already showed the importance of packing. With the complete model, this effect still remains effective. Finally the role of the adhesion energy $\alpha$ (between cells and the matrix) was more tricky but eventually was found to play a role, in particular when $\alpha/R$ becomes comparable with the other moduli, i.e. cell ($G_i$) and collagen ones ($G_m$). This was particularly noticeable at the lowest frequencies used in the experiments (Fig.6). A more elastic behavior (higher elastic plateau and higher transition frequency) was observed corresponding to higher values of the adhesion energy. This was also observed in an earlier work on polymer emulsions[37] reporting the relevance of this parameter only at lower frequencies, when the terminal relaxation time scales with interfacial tension. To study further the importance of this feature, other more complex models including poroelastic effects may also be needed in the future[47].

After analyzing the results on three different spheroids[18], prepared with various initial collagen concentrations ($c_0$ = 0 mg/mL, 0.01 mg/mL and 0.03 mg/mL) we used the emulsion model to optimize the parameters and came up with the best possible fits (Fig. 7 and Table 2). The results of the model were found to be in very good agreement with the experiments. We noted a small discrepancy for the case of the spheroids prepared without collagen ($c_0$ = 0 mg/mL). This could be explained by the absence of a dense structure as exhibited on the confocal images (Fig. 3). Still the agreement found was interesting as it motivates further effects in view of the parameters investigated. In particular, the packing of cells within the spheroid seems to be linked with the presence of collagen forming a dense meshwork, enabling cells to connect with each others, in the presence of adhesion molecules (cadherins for instance[48]). Indeed, the optimal adhesion energy increased with $c_0$, the initial collagen content (see Table 2), ranging from 30 to 80 mN/m. In addition, an increase in the initial collagen content was found to enhance cell packing (higher value of $\phi$) – which was rather unexpected – this giving rise to higher viscoelastic moduli (see Figs 1-2).

To go beyond this result, we can analyse the ability of the model to predict various slopes, like the ones observed experimentally for cells[26,32,49–52] and spheroids[6,18]. The dependence on frequency at low rates is usually weak for cells or ECM (slopes typically 0.1–0.3), whereas it can become larger at higher frequencies (slope $\sim$ 1 for G") with a possible exponent of 0.5 for poroelastic materials[13]. The slopes found here using the model correspond to the complex combination of the viscoelastic properties of both the ECM and the cell's properties. Thus the model predicts a rich variety of spheroid viscoelastic properties, and power–law dependencies[33]. Hence it would be interesting to study spheroids in more in detail in the future, for example when using various cell types or ECM leading to different microstructures[53], or during the growth of tumours[40,42,43]. These microstructures should be minutely analyzed further using confocal microscopy at smaller scales, in order to extract the basic relationships or forces involved in such interactions, in particular since we noticed the effect of the adhesion energy here. Finally another important fact is that cells can pull on the collagen to generate forces or remodel it[25]. This can lead to a stiffening of the matrix if large deformations are reached, and this could eventually change the spheroid properties. As far as small deformations are considered, the model can still apply but may show some limitations if larger deformations are involved.

## 7 Conclusions

The rheology of spheroids has insufficiently been studied so far. Here we used previous viscoelastic data on spheroids measured with an AFM, as well as the individual response of the other components (i.e. cells and collagen). Results were compared with the predictions of an emulsion model including interfacial energy. The results were in very good agreement with the experiments. They showed that the final spheroid microstructure contains dense collagen regions within the inter-cellular spacing. Finally an increased initial collagen concentration led to an an enhanced compactness of the spheroids with a smaller inter-cellular spacing, and a larger adhesion energy. Thus collagen plays the role of a connecting adhesive layer between the cells and improves spheroid stability. With this model, future predictions regarding time–dependent spheroid growth should be possible.

## Author Contributions

C.V. carried out single cell and collagen experiments, data analysis and simulations. Both authors designed research and wrote the manuscript.

## Conflicts of interest

There are no conflicts to declare.

## Acknowledgements

The authors are thankful to the Nanoscience Foundation (Grenoble) for sponsoring the AFM. C.V. is a member of the LabeX Tec 21, France (Investissements d'Avenir: grant agreement No. ANR-11-LABX-0030). The authors thank D. Tsvirkun for help with the spheroids preparation needed to test single cells, and J. Revilloud for interesting discussions.

## Notes and references

1 L.-B. Weiswald, D. Bellet and V. Dangles-Marie, *Neoplasia*, 2015, **17**, 1–15.

2 M. Delarue, F. Montel, D. Vignjevic, J. Prost, J.-F. Joanny and G. Cappello, *Biophys. J.*, 2014, **107**, 1821–1828.

3 D. Ambrosi, S. Pezzuto, D. Riccobelli, T. Stylianopoulos and P. Ciarletta, *J. Elasticity*, 2017, **129**, 107–124.

4 L. Guillaume, L. Rigal, J. Fehrenbach, C. Severac, B. Ducommun and V. Lobjois, *Sci. Rep.*, 2019, **9**, 6597.

5 M. Dolega, G. Zurlo, M. L. Goff, M. Greda, C. Verdier, J.-F. Joanny, G. Cappello and P. Recho, *J. Mech. Phys. Solids*, 2021, **147**, 104205.

6 Y. Abidine, A. Giannetti, J. Revilloud, V. M. Laurent and C. Verdier, *Cells*, 2021, **10**, 1704.

7 L. Preziosi, D. Ambrosi and C. Verdier, *J. Theor. Biol.*, 2010, **262**, 35–47.

8 M. Lekka, P. Laidler, D. Gil, J. Lekki, Z. Stachura and A. Z. Hrynkiewicz, *Eur. Biophys. J.*, 1999, **28**, 312–316.

9 S. E. Cross, Y.-S. Jin, J. Rao and J. K. Gimzewski, *Nat. Nanotechnol.*, 2007, **2**, 780–783.

10 M. Plodinec, M. Loparic, C. A. Monnier, E. C. Obermann, R. Zanetti-Dallenbach, P. Oertle, J. T. Hyotyla, U. Aebi, M. Bentires-Alj, R. Y. H. Lim and C.-A. Schoenenberger, *Nat. Nanotechnol.*, 2012, **7**, 757–765.

11 J. Rother, H. Nöding, I. Mey and A. Janshoff, *Open Biology*, 2014, **4**, 140046.

12 K. Gnanachandran, S. Kędracka-Krok, J. Pabijan and M. Lekka, *J. Biomech.*, 2022, **144**, 111346.

13 J.-T. Hang, G.-K. Xu and H. Gao, *Sci. Adv.*, 2022, **8**, eabn6093.

14 J. Solon, I. Levental, K. Sengupta, P. C. Georges and P. A. Janmey, *Biophys. J.*, 2007, **93**, 4453–4461.

15 C. T. Mierke, *Rep. Prog. Phys.*, 2019, **82**, 064602.

16 M. E. Dolega, S. Monnier, B. Brunel, J.-F. Joanny, P. Recho and G. Cappello, *eLife*, 2021, **10**, 1–33.

17 P. A. Netti, S. Roberge, Y. Boucher, L. T. Baxter and R. K. Jain, *Microvasc. Res.*, 1996, **52**, 27–46.

18 D. Tsvirkun, J. Revilloud, A. Giannetti and C. Verdier, *J. Biomech.*, 2022, **141**, 111229.

19 B. R. Dasgupta and D. A. Weitz, *Phys. Rev. E*, 2005, **71**, 021504.

20 P. A. Janmey, M. E. McCormick, S. Rammensee, J. L. Leight, P. C. Georges and F. C. MacKintosh, *Nat. Mater.*, 2007, **6**, 48–51.

21 D. Vader, A. Kabla, D. Weitz and L. Mahadevan, *PLoS One*, 2009, **4**, e5902.

22 C. P. Broedersz, K. E. Kasz, L. M. Jawerth, S. Munster, D. A. Weitz and F. C. MacKintosh, *Soft Matter*, 2010, **6**, 4120–4127.

23 F. Sauer, L. Oswald, A. Ariza de Schellenberger, H. Tzschätzsch, F. Schrank, T. Fischer, J. Braun, C. T. Mierke, R. Valiullin, I. Sack and J. A. Käs, *Soft Matter*, 2019, **15**, 3055–3064.

24 K. L. Goh, J. R. Meakin, R. M. Aspden and D. W. L. Hukins, *J. Theor. Biol.*, 2007, **245**, 305–311.

25 A. Iordan, A. Duperray, A. Gérard, A. Grichine and C. Verdier, *Biorheology*, 2010, **47**, 277–295.

26 J. Alcaraz, L. Buscemi, M. Grabulosa, X. Trepat, B. Fabry, R. Farré and D. Navajas, *Biophys. J.*, 2003, **84**, 2071–2079.

27 Y. Abidine, V. M. Laurent, R. Michel, A. Duperray, L. I. Palade and C. Verdier, *Europhys. Letters*, 2015, **109**, 38003.

28 T. Boudou, J. Ohayon, Y. Arntz, G. Finet, C. Picart and P. Tracqui, *J. Biomech.*, 2006, 1677–1685, volume = 39, owner = claude, timestamp = 2007.02.26,.

29 Z. Kalcioglu, R. Mahmoodian, Y. Hu, Z. Suo and K. V. Vliet, *Soft Matter*, 2012, **8**, 3393–3398.

30 F. Gittes, B. Schnurr, P. Olmsted, F. MacKintosh and C. Schmidt, *Phys. Rev. Letters*, 1997, **79**, 3286–3289.

31 E. Moeendarbary, L. Valon, M. Fritzsche, D. M. A.R. Harris, A. Thrasher, E. Stride, L. Mahadevan and G. T. Charras, *Nat. Mater.*, 2013, **12**, 253–261.

32 Y. Abidine, A. Constantinescu, V. M. Laurent, V. S. Rajan, R. Michel, V. Laplaud, A. Duperray and C. Verdier, *Biophys. J.*, 2018, **114**, 1165–1175.

33 P. Sollich, F. Lequeux, P. Hébraud and M. E. Cates, *Phys. Rev. Lett.*, 1997, **78**, 2020–2023.

34 G. Massiera, K. M. V. Citters, P. L. Biancaniello and J. C. Crocker, *Biophys. J.*, 2007, **93**, 3703–3713.

35 J.-F. Palierne, *Rheol. Acta*, 1990, **29**, 204–214.

36 J.-F. Palierne, *Rheol. Acta*, 1991, **30**, 497.

37 D. Graebling, R. Müller and J.-F. Palierne, *Macromolecules*, 1993, **26**, 320–329.

38 A. Einstein, *Annals der Physik*, 1911, **34**, 591–592.

39 H. Nia, I. Bozchalooi, Y. Li, L. Han, H.-H. Hung, E. Frank, K. Youcef-Toumi, C. Ortiz and A. Grodzinsky, *Biophys. J.*, 2013, **104**, 1529–1537.

40 G. Helmlinger, P. A. Netti, H. C. Lichtenbeld, R. J. Melder and R. K. Jain, *Nat. Biotechnol.*, 1997, **15**, 778–783.

41 H. Byrne and L. Preziosi, *Math. Med. Biol.*, 2003, **20**, 341–366.

42 T. Stylianopoulos, J. D. Martin, V. P. Chauhan, S. R. Jain, B. Diop-Frimpong, N. Bardeesy, B. L. Smith, C. R. Ferrone, F. J. Hornicek, Y. Boucher, L. L. Munn and R. K. Jain, *Proc. Natl Acad. Sci. USA*, 2012, **109**, 15101–15108.

43 D. Ambrosi, L. Preziosi and G. Vitale, *Mech. Res. Commun.*, 2012, **42**, 87–91.

44 P. P. Provenzano, K. W. Eliceiri, J. M. Campbell, D. R. Inman, J. G. White and P. J. Keely, *BMC Medicine*, 2006, **4**, 38.

45 C. J. Whatcott, C. H. Diep, P. Jiang, A. Watanabe, J. LoBello, C. Sima, G. Hostetter, H. M. Shepard, D. D. Von Hoff and H. Han, *Clin. Cancer Res.*, 2015, **21**, 3561–3568.

46 M. Brooks, Q. Mo, R. Krasnow, P. L. Ho, Y.-C. Lee, J. Xiao, A. Kurtova, S. Lerner, G. Godoy, W. Jian, P. Castro, F. Chen, D. Rowley, M. Ittmann and K. S. Chan, *Oncotarget*, 2016, **7**, 82609–82619.

47 P. Royer, P. Recho and C. Verdier, *Mech. Res. Commun.*, 2019, **96**, 19–23.

48 E. M. Bindels, M. Vermey, R. van den Beemd, W. N. Dinjens and T. H. V. D. Kwast, *Cancer Res.*, 2000, **60**, 177–183.

49 L. Deng, X. Trepat, J. P. Butler, E. Millet, K. G. Morgan, D. A. Weitz and J. J. Fredberg, *Nat. Mater.*, 2006, **5**, 636–640.

50 P. Bursac, B. Fabry, X. Trepat, G. Lenormand, J. P. Butler, N. Wang, J. J. Fredberg and S. S. An, *Biochem. Biophys. Res. Commun.*, 2007, **355**, 324–330.

51 D. Stamenovic, N. Rosenblatt, M. Montoya-Zavala, B. D. Matthews, S. Hu, B. Suki, N. Wang and D. E. Ingber, *Biophys. J.*, 2007, **93**, L39–L41.

52 P. Cai, Y. Mizutani, M. Tsuchiya, J. M. Maloney, B. Fabry, K. J. V. Vliet and T. Okajima, *Biophys. J.*, 2013, **105**, 1093–1102.

53 G. Quarto, L. Spinelli, A. Pifferi, A. Torricelli, R. Cubeddu, F. Abbate, N. Balestreri, S. Menna, E. Cassano and P. Taroni, *Biomed. Opt. Express*, 2014, **5**, 3684–3698.